

Survival of Bundleless Hair Cells and Subsequent Bundle Replacement in the Bullfrog's Sacculle

Jonathan E. Gale,^{1*} Jason R. Meyers,¹ Ammasi Periasamy,² Jeffrey T. Corwin¹

¹ Department of Otolaryngology, HNS and Department of Neuroscience, University of Virginia School of Medicine, Charlottesville, Virginia 22908

² Department of Biology, Keck Center for Cellular Imaging, University of Virginia, Charlottesville, Virginia 22906

Received 29 May 2001; accepted 12 July 2001

ABSTRACT: Our senses of hearing and balance depend upon hair cells, the sensory receptors of the inner ear. Millions of people suffer from hearing and balance deficits caused by damage to hair cells as a result of exposure to noise, aminoglycoside antibiotics, and antitumor drugs. In some species such damage can be reversed through the production of new cells. This proliferative response is limited in mammals but it has been hypothesized that damaged hair cells might survive and undergo intracellular repair. We examined the fate of bullfrog saccular hair cells after exposure to a low dose of the aminoglycoside antibiotic gentamicin to determine whether hair cells could survive such treatment and subsequently be repaired. In organ cultures of the bullfrog sacculle a combination of time-lapse video microscopy, two-photon microscopy, electron microscopy, and immunocytochemistry showed that hair cells can

lose their hair bundle and survive as bundleless cells for at least 1 week. Time-lapse and electron microscopy revealed stages in the separation of the bundle from the cell body. Scanning electron microscopy (SEM) of cultures fixed 2, 4, and 7 days after antibiotic treatment showed that numerous new hair bundles were produced between 4 and 7 days of culture. Further examination revealed hair cells with small repaired hair bundles alongside damaged remnants of larger surviving bundles. The results indicate that sensory hair cells can undergo intracellular self-repair in the absence of mitosis, offering new possibilities for functional hair cell recovery and an explanation for non-proliferative recovery. © 2002 John Wiley & Sons, Inc. *J Neurobiol* 50: 81–92, 2002; DOI 10.1002/neu.10002

Keywords: vestibular; repair; regeneration; deafness; hearing; ototoxicity

INTRODUCTION

Hair cells are the sensory receptor cells of the inner ear that transduce mechanical stimuli into electrical

activity (Hudspeth, 1989; Ashmore and Gale, 2000). Loss of hair cells is the major cause of noncongenital hearing and balance deficits (Nadol, 1993), and damage to the transduction apparatus, the stereocilia bundle on the surface of the hair cell, is sufficient to cause hearing deficits (Liberman and Dodds, 1984).

Research in rodents has indicated that hair cells in mammalian ears are normally produced only during embryonic and neonatal development (Ruben, 1967), so that nearly all forms of damage to mammalian hair cells have been considered irreversible, consistent with the clinical permanence of hearing deficits (Lambert, 1994). That is not the case, however, for non-mammalian vertebrates. In fish and amphibians, thousands of hair cells are added to the ear throughout normal life, and lost hair cells are replaced (Corwin, 1981, 1983, 1985; Popper and Hoxter, 1984; Diaz et

* Present address: Department of Physiology, University College London, Gower Street, London, WC1E 6BT, U.K.

Correspondence to: J. Gale (j.e.gale@ucl.ac.uk) or J. T. Corwin (jcorwin@virginia.edu).

Contract grant sponsor: National Institute on Deafness and Other Communication Disorders; contract grant number: RO1-0200.

Contract grant sponsor: National Organization for Hearing Research.

Contract grant sponsor: Lions of Virginia Hearing Research Center and Foundation.

Contract grant sponsor: Wellcome Trust Prize Travelling Fellowship (J.E.G.).

© 2002 John Wiley & Sons, Inc.

al., 1995). In birds, damage to the ear can be repaired in less than 2 weeks via trauma-evoked production of new hair cells (reviewed in Corwin and Oberholtzer, 1997).

Recently it was discovered that vestibular epithelia in mammalian ears exhibit some recovery after antibiotic damage and that the machinery for regenerative proliferation could operate at a low level in mammalian ears (Forge et al., 1993; Warchol et al., 1993). However, the incidence of cell proliferation *in vitro* was lower than might have been expected from the incidence of immature hair bundles that appeared *in vivo* after damage, suggesting that mechanisms independent of regenerative proliferation were involved. Recent work that utilized low doses of aminoglycoside antibiotics has suggested that the replacement of hair cells can occur in the absence of mitosis in non-mammalian (Adler and Raphael, 1996; Baird et al., 1996; Roberson et al., 1996) and mammalian systems (Li and Forge, 1997; Zheng et al., 1999). Thus, it has been suggested that replacement hair cells could arise via conversion of cells from a supporting cell phenotype into a hair cell phenotype. An alternative hypothesis is that damaged hair cells might survive and undergo cellular repair (Corwin et al., 1996). There is some evidence consistent with such self-repair in damaged mammalian epithelia (Sobkowicz et al., 1997; Zheng et al., 1999), but it remained to be determined how hair cells might lose their hair bundles and whether the same cells then reform a new transduction apparatus.

We set out to test the hypothesis that hair cells could lose their apical components, survive in the epithelium, and then rebuild their hair bundle. We treated bullfrog saccules with a low dose of aminoglycoside antibiotics for 16–18 h and undertook long-term time-lapse and two-photon microscopic recordings in order to follow the damage and recovery of the hair cells. We also used scanning and transmission electron microscopy (SEM and TEM) as well as immunocytochemistry in determining how the damage and recovery processes proceeded.

MATERIALS AND METHODS

Organ Culture

Sixty-five bullfrog (*Rana catesbiana*) saccules were dissected in HEPES-buffered frog Ringer's (pH 7.25, 110 mM NaCl, 2 mM KCl, 3 mM glucose, 10 mM HEPES) containing 0.1 mM calcium chloride, then placed in 50 $\mu\text{g}/\text{mL}$ subtilisin (protease type VIII; Sigma, USA) in calcium-free frog Ringer's for 15 min. The otolithic membrane was then removed using a gentle flow of Ringer's. The organs were

placed in a 30 μL collagen droplet and cultured in Wolf and Quimby medium (Gibco, USA) with added sodium pyruvate (100 μM), 1X nonessential MEM amino acid solution (Gibco), and the antibiotic ciprofloxacin (0.01%) based on the method of Baird et al. (1996). Test saccules were placed in culture medium supplemented with 300 μM gentamicin for 16–18 h and then the media in treated and control cultures were replaced with fresh control medium. Medium was changed every 48–72 h. Saccules for electron microscopic analysis, time-lapse, and two-photon time-series experiments were cultured in the presence of the DNA polymerase inhibitor aphidicolin at 25 μM (Harris and Hartenstein, 1991).

Time-Lapse and Two-Photon Imaging

For time-lapse recordings saccules were cultured as above except that they were oriented with their hair bundles down in collagen droplets and placed in Rose chambers on an inverted microscope at 24–26°C. The microscope was under software control (Metamorph; Universal Imaging Inc., USA) allowing up to 12 *z*-axis focal planes to be recorded (typically only three were) in concurrent time lapse over a 4–10 day period. Images were acquired every 3 to 5 min typically covering a *z* depth of between 30 and 45 μm . Saccules used for two-photon fluorescence microscopy were incubated for 5 min in 30 μM FM1-43 (Molecular Probes, USA), which loads into bullfrog hair cells selectively (Gale et al., 2000), in HEPES-buffered frog Ringer's and then were prepared as they were for time-lapse recordings. Images were acquired every 24 h starting at the end of the gentamicin treatment. Image stacks were obtained using two-photon excitation at 870 nm in a laser scanning confocal microscope (Periasamy et al., 1999). Stacked *z*-section images were acquired at 0.5 μm intervals starting above the level of the hair bundles and ending below the bottom of the epithelium. Image stacks were taken from the same regions in the saccules at 24 h intervals starting at the end of the 16–18 h gentamicin treatment. *xz* views of the epithelium were reconstructed from 120–140 individual two-photon sections of the epithelium.

Immunocytochemistry

Thirty-six saccules, 12 each at 2, 4, and 7 days post-treatment, were placed in medium containing 1 μM ethidium homodimer, a marker of dead cells (Molecular Probes), for 30 min to test for cell death. To positively confirm the viability of surviving cells 2 days after the antibiotic treatment, two saccules were placed in medium that contained 1 μM Calcein-AM (Molecular Probes), which is cleaved by esterases and is thus a marker of live cells.

The hair cell antibody, HCS-1, was generated by immunizing mice with sensory epithelia isolated from the utricles of 1- to 21-day-old White Leghorn chicks. The monoclonal antibody HCS-1 binds specifically to the cell bodies of hair cells in inner ear tissues from rat, mouse, chick, frog, and

shark (Gale et al., 2000; Finley et al., 1997). Specimens were incubated in purified antibody (1:1000) in PBS with 5% normal goat serum and 0.1% Triton X-100 overnight at 4°C, followed by Cy3-conjugated goat antimouse IgG secondary antibody (1:200; Jackson Laboratories, USA). To visualize filamentous actin, FITC-conjugated phalloidin (Sigma) was used at 0.5 $\mu\text{g}/\text{mL}$ for 1 h at room temperature. Nuclei were visualized with the DNA stain DAPI (Molecular Probes). Specimens were mounted in Fluoromount-G (Southern Biotechnology, AL) and viewed using epifluorescence microscopy. HCS-1 positive cells were counted in three 10,000 μm^2 regions per sacculle using Metamorph imaging software.

Electron Microscopy

Thirty-five cultures fixed 2, 4, or 7 days after gentamicin treatment were prepared for electron microscopy. Specimens were prefixed with 1% OsO_4 for 10 min and then fixed in 2% glutaraldehyde/2% paraformaldehyde in 0.1 M sodium cacodylate, pH 7.4. Thin sections were stained with 1% aqueous uranyl acetate. SEM samples were prepared by ligand binding of osmium with thiocarbonylhydrazide before critical point drying. A minimum of six sacculles were examined by SEM at each time point. Bundle counts from SEM samples were made from six separate 4,180 μm^2 regions in the center of the macula of each sacculle. Hair bundles were classified as surviving, extruding, small, or “blackholes” (cell surfaces that often had one short cilium but few, if any, microvilli and no stereocilia). Intermediate sized bundles that may have been pre-existing were tabulated as unclassified.

In order to correct for tissue shrinkage during processing for SEM, we measured the surface diameters of supporting cells in paraformaldehyde-fixed whole mounts ($5.9 \pm 0.1 \mu\text{m}$, mean \pm S.E.M.) and compared them to SEM preparations ($4.3 \pm 0.1 \mu\text{m}$, $n = 40$). The difference in variance between the data sets was less than 2%. Thus, our estimate for the diameter change due to tissue shrinkage was 27%, and we applied this correction to our calculations of bundle density from SEM preparations.

RESULTS

We examined saccular cultures 2, 4, and 7 days after an 18 h treatment with 300 μM gentamicin by labeling with HCS-1 (Gale et al., 2000) and FITC-phalloidin. Counts of HCS-1 positive hair cells showed that many died after the gentamicin treatment, but many others survived. FITC-phalloidin staining of f-actin revealed hair bundles that had survived the gentamicin treatment and showed numerous bundles that were damaged by the aminoglycoside treatment. We also found HCS-1 positive cells that had no hair bundles at their surfaces, which we term bundleless hair cells [Fig. 1(A)]. After gentamicin, we observed bundleless

cells at all time points examined [Fig. 1(B), arrow]. Damaged hair cells exhibited abnormal cell shapes, with processes extending up to 10 μm from the cell body [Fig. 1(C)]. This cell morphology contrasted sharply with that of undamaged hair cells, which remained cylindrical.

In order to label dead cells, sets of 12 sacculles were incubated in ethidium homodimer at 2, 4, and 7 days after the gentamicin treatment. The sensory epithelia typically contained less than 10 dead cells at 2 days and no dead cells at 4 and 7 days (data not shown). In the latter cases dead cells were found outside the macula, confirming that ethidium was labeling properly. Cellular viability was also confirmed by positive staining in two sacculles treated with Calcein-AM, which is cleaved by esterases and is thus trapped in live cells. The sacculles that were treated with ethidium were then fixed and double-labeled with FITC-phalloidin and the HCS-1 antibody. The combination of positive labeling with HCS-1, the absence of labeling with ethidium homodimer, and the absence of phalloidin-stained hair bundles demonstrated that bundleless hair cells survived for at least 7 days [Fig. 1(A,B)].

In order to investigate whether new hair bundles might arise in the absence of cell proliferation we used aphidicolin, a DNA polymerase inhibitor (Harris and Hartenstein, 1991). To find the concentration of aphidicolin at which cell proliferation was completely blocked, we cultured six sacculles for 7 days in media containing BrdU in aphidicolin at 10, 25, and 50 μM . Staining with an anti-BrdU antibody (1:60; Becton Dickinson, CA) revealed that 25 μM aphidicolin completely blocked progress through S-phase (data not shown). All subsequent cultures for electron microscopy, time-lapse, and two-photon time-series experiments contained 25 μM aphidicolin.

To determine how the bundleless cells originated we monitored the saccular epithelium in continuous time-lapse microscopy at high magnification during and after low-dose gentamicin treatment. Tilting of the normally upright hair bundles was an early sign of gentamicin's effect on the hair cells that eventually lost their bundles [Figs. 2(A,B) and 3(A)]. Upward extrusion of the cell surface and lateral displacement of the bundle followed the tilting [Figs. 2(C) and 3(B)]. Blebbing, splaying, and disarray of some stereocilia occurred during extrusion of the apical surface. A few hair bundles separated in a way that suggested the cuticular plate had split [Fig. 2(F,G)]. In those cases, one part of the split bundle tilted and extruded from the cell, while the rest of the hair bundle remained in its normal position [Fig. 2(H)]. Tilting and extrusion typically began during the gen-

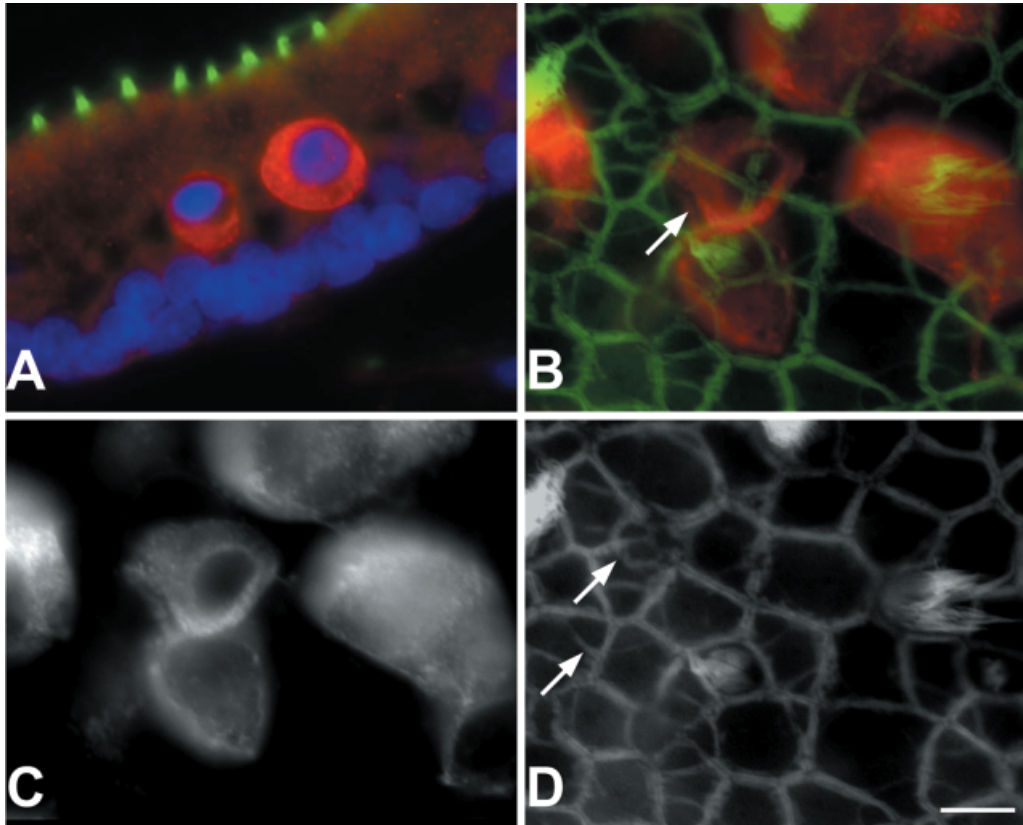


Figure 1 Hair cells survive within the sensory epithelium without hair bundles. (A) A $7\ \mu\text{m}$ thick cross-section of the epithelium 4 days after the end of gentamicin treatment labeled with the HCS-1 antibody (red), phalloidin (green), and DAPI (blue). Two bundleless hair cells can be seen below the surface of the epithelium. Serial sections confirmed that these hair cells did not reach the epithelium's surface. The hair cell nuclei lie above the nuclei of the supporting cells that form a single layer just above the basal lamina. Filamentous actin in the circumferential rings beneath the apical surfaces of supporting cells is seen in a slightly tangential section, but there were no actin hair bundles found above the hair cells. (B) A double-labeled image from a whole mount, revealing hair cell bodies (red) and filamentous actin in the stereocilia of hair bundles (green). A surviving hair cell with a hair bundle can be seen adjacent to a hair cell that has lost its apical hair bundle (arrow). (C) Labeling of hair cell bodies with HCS-1. (D) Phalloidin labeling shows damaged yet surviving hair bundles as well as the subapical filamentous actin rings in the supporting cells. The surface scar pattern (arrows) resulting from supporting cell invasion indicates that the cell underneath the surface [in (B)] has lost its hair bundle. Scale bars: $10\ \mu\text{m}$.

tamicin treatment and continued for up to 72 h. Time-lapse sequences showed the hair cells' apices separating from some cells by constriction of the cell bodies just beneath the epithelium's surface [Fig. 2(C)]. The process progressed until the constricting hair cells' outlines disappeared from the focal plane just below the surface. During this period the hair bundles and cell bodies remained clearly visible in concurrent image sequences from the surface focal plane and focal planes deeper in the epithelium in the z -axis series [Fig. 2(D)]. From the onset of surface bleb formation to the complete separation, the subsurface constriction took 135 ± 21 min (mean \pm S.E.M., n

$= 12$). Hair cells undergoing cell death, presumably via apoptosis (Li et al., 1995), were also observed in the time-lapse recordings. The complete extrusion of the cell bodies of the dying cells contrasted sharply with the images of other cells in the same fields that lost only their hair bundles and small volumes of apical cytoplasm.

To follow events in labeled living hair cells in three dimensions, we used FM1-43, a styryl dye that specifically loads into bullfrog saccular hair cells (Gale et al., 2000), and monitored gentamicin-treated saccules using two-photon confocal microscopy [Fig. 2(I)]. Stacks of z -sections were obtained

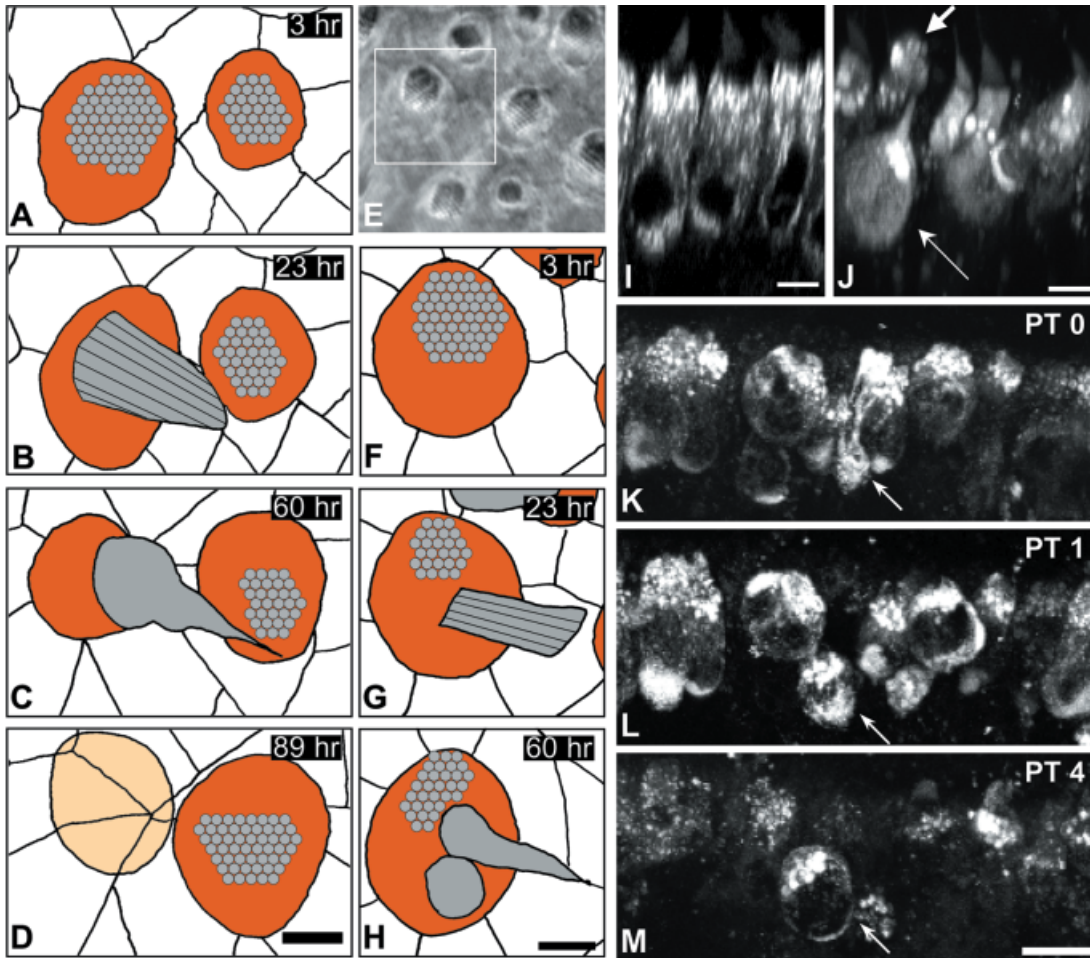


Figure 2 Separation of hair bundles from cell bodies after gentamicin treatment. (A–D) Tracings of four consecutive time-lapse images. The time after the end of the aminoglycoside treatment is indicated (upper right). Hair bundles are shown in grey and the hair cell surfaces in orange. The circles represent a schematic pattern of stereocilia in the hair bundle rather than individual stereocilia. (A) At the beginning of the time-lapse, the hair bundles are upright and intact. (B) At 23 hours, the hair bundle of the cell on the left has tilted over. (C) At 60 hours the left hair bundle has been displaced and apical cytoplasm has extruded above the epithelial surface. (D) At 89 hours, the neighboring supporting cells have covered over the site that was previously occupied by the hair cell. The hair cell body remained deeper in the epithelium (indicated by pale orange shading). (E) A single video frame from the same time-lapse recording. The region traced in F is outlined. F–H are tracings showing a hair cell in which the hair bundle was split and subsequently only a part of hair bundle was lost. (I) FM1-43 loads into hair cells selectively. Multi-photon XZ reconstruction of a living frog sacculle loaded with $30 \mu\text{M}$ FM1-43. (J) XZ reconstruction shortly after the end of gentamicin treatment. A hair cell can be seen separating from its hair bundle (arrow). (K–M) A time series of XZ reconstructions. (K) At post-treatment day zero (PT 0) one damaged hair cell (thin arrow) is observed along with extruded cytoplasm at the surface (thick arrow). (L) At PT 1 the cell is observed as a bundle-less hair cell below the surface of the epithelium (arrow). The same cell survives without its hair bundle until at least PT 4 (M). The same cell was still present in the epithelium at PT 6 at which point the experiment was terminated. Scale bars: (A–H) $2 \mu\text{m}$, (J and K) $5 \mu\text{m}$, (K–M) $5 \mu\text{m}$.

for the selected regions of the sacculle every 24 h after the end of the gentamicin treatment. Three-dimensional reconstructions revealed hair cells in

the process of separating from their bundles [Fig. 2(J), arrows] as well as cells that had lost their bundles and survived as bundleless cells [Fig. 2(K–

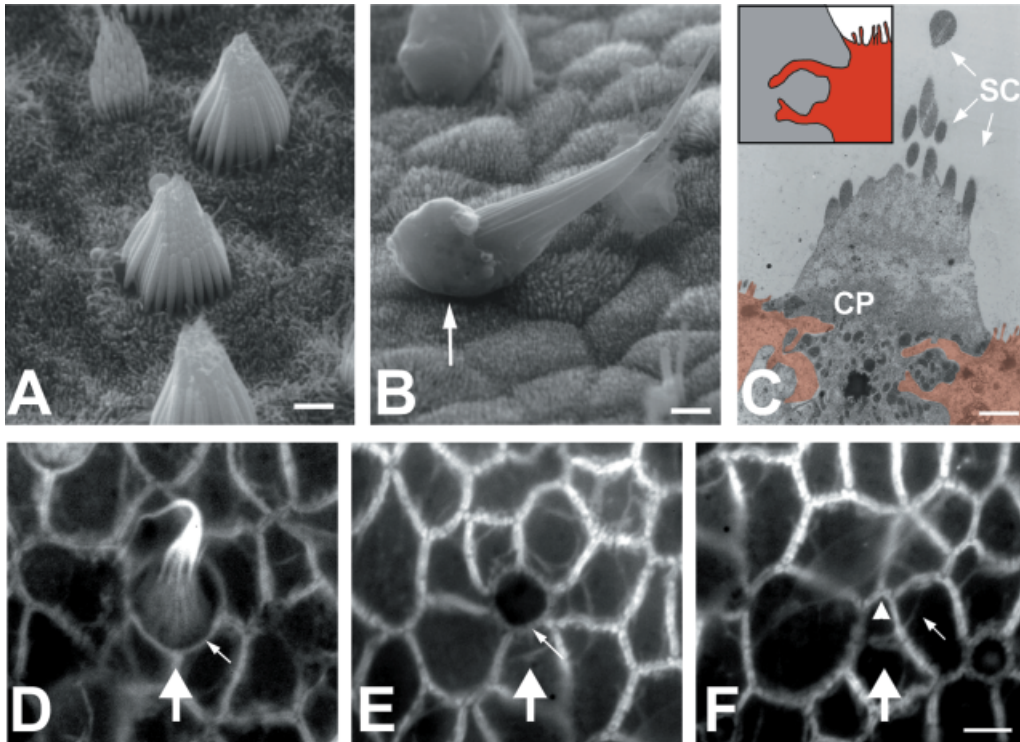


Figure 3 Changes at the surface of the sensory epithelium. (A) A scanning electron micrograph of hair bundles at the surface of a control saccule reveals the normal organization of the hair bundles. (B) Micrograph taken 2 days after gentamicin treatment. An extruded hair bundle with part of the cell's apical cytoplasm attached rests on the surface of the epithelium. (C) A transmission electron micrograph of a saccule fixed 2 days after gentamicin treatment during the process of hair bundle separation. Fingerlike processes from adjacent supporting cells can be seen extending into a hair cell. The processes extend just beneath the dense cuticular plate (CP) and the vertically displaced stereocilia (SC) in the hair bundle. The inset shows a tracing indicating the supporting cell processes (red) that project into the body of the hair cell (dark gray). (D–F) Scar formation at the epithelial surface. Phalloidin staining reveals filamentous actin in the cortical network at the surface of the epithelium. Three images from different areas of the same specimen. The thick arrow indicates the region of scar formation. (D) A surviving hair cell with a dense actin ring where the adherens junctions are formed between the hair cell and supporting cells (thin arrow). (E) The surfaces of the surrounding supporting cells invade in to seal the epithelium, observed as a constriction of the subsurface actin ring (thin arrow). (F) Neighboring supporting cells have sealed over the surface (arrowhead). A weakly labeled circular actin ring remains that appears to be comprised of a single segment of filamentous actin in each supporting cell that originally resided near the junction with the hair cell (thin arrow). Scale bars: (A, B, and C) 1 μm , (D, E, and F) 5 μm .

M), arrows]. Bundleless cells were observed to survive for at least 6 days, the longest time point we could examine, which is consistent with the observations that HCS-1 positive cells without bundles were found in fixed specimens 7 days after the end of the gentamicin treatment.

Using SEM and TEM we examined cultured saccules fixed 2 days after the end of the gentamicin treatment to look for cells in the process of losing their hair bundles. In contrast to undamaged saccular hair cells [Fig. 3(A)], many hair cells in gentamicin-treated cultures showed tilted hair bundles with fused

stereocilia that were clearly damaged. In some cases the apical poles of hair cells were observed lying on the surface of the epithelium separated from the cell bodies [Fig. 3(B), arrow]. In thin sections we observed narrow fingers of supporting cell cytoplasm that extended beneath the extruding hair bundle and cuticular plate [Fig. 3(C)]. In the cell shown in Figure 3(C), the stereocilia were partially fused, and the cuticular plate appeared to be extruding above the epithelial surface. The invading cytoplasmic fingers were close to the adherens junction, where a circumferential ring of f-actin lies in both hair cells and

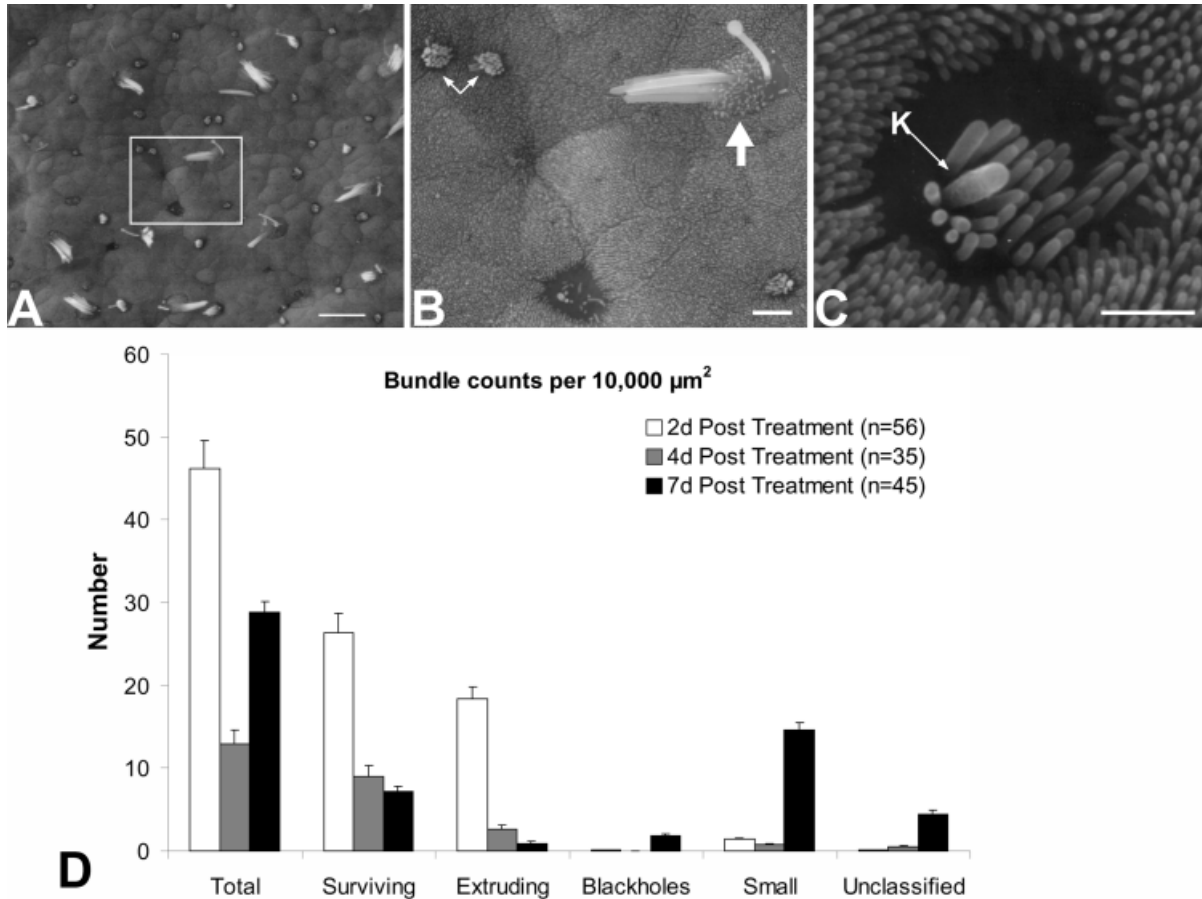


Figure 4 Scanning electron micrographs of damaged saccular epithelia 7 days after gentamicin treatment. (A) A low magnification view of the surface of a sacculle fixed 7 days after gentamicin treatment. A number of larger, damaged, surviving bundles can be seen across the width of the epithelium along with numerous small, immature-like bundles. (B) A higher magnification view of the boxed area in (A). A pair of small, apparently immature bundles (thin arrows) and a damaged, surviving hair bundle (thick arrow) are visible in the top half of the micrograph. A “black hole” (lower left) and single small hair bundle (to the right) are visible in the bottom half. (C) A small, immature appearing bundle viewed at high magnification. The new bundle has short, thin stereocilia and a kinocilium (K) recognizable by its greater diameter and height. (D) Hair bundle counts from SEM preparations. All values given are means \pm S.E.M., n = the number of 4,180 μm^2 regions counted. Scale bars: (A) 10 μm , (B) 2 μm , (C) 1 μm .

supporting cells (Flock et al., 1981). When gentamicin-treated sacculles were fixed and stained with FITC-phalloidin, cells could be observed at different stages during the constriction of their actin belts with the resultant formation of scars at the surface of the epithelium [Fig. 3(D–F), arrow].

In addition, we undertook a detailed study of the epithelial surfaces of 24 cultured sacculles using SEM. We observed hair bundles with tilted, fused, and missing stereocilia [Fig. 4(A), thick arrow in (B)], as well as detached hair bundles lying on the surface of the epithelium [Fig. 3(B), arrow]. Damaged hair bundles were seen at 2, 4, and 7 days after gentamicin treatment, and SEM showed rather dramatic surface

changes in hair bundle form as the sacculles recovered. The numbers of large bundles declined from 26 per 10,000 μm^2 at 2 days after the gentamicin treatment to 7 per 10,000 μm^2 at 7 days. At 4- and 7-day time points, most of the large bundles had abnormal morphology, with tilted and fused stereocilia, indicating damage from the gentamicin treatment. Bundles with membranous blebs visible above the surface were tabulated as extruding from the sensory epithelium. The numbers of extruding bundles declined from 18 per 10,000 μm^2 at 2 days to 1 per 10,000 μm^2 at 7 days. Smooth cell surfaces (which we termed “blackholes”), devoid of a hair bundle or microvilli but often having a single eccentrically positioned kinocilium,

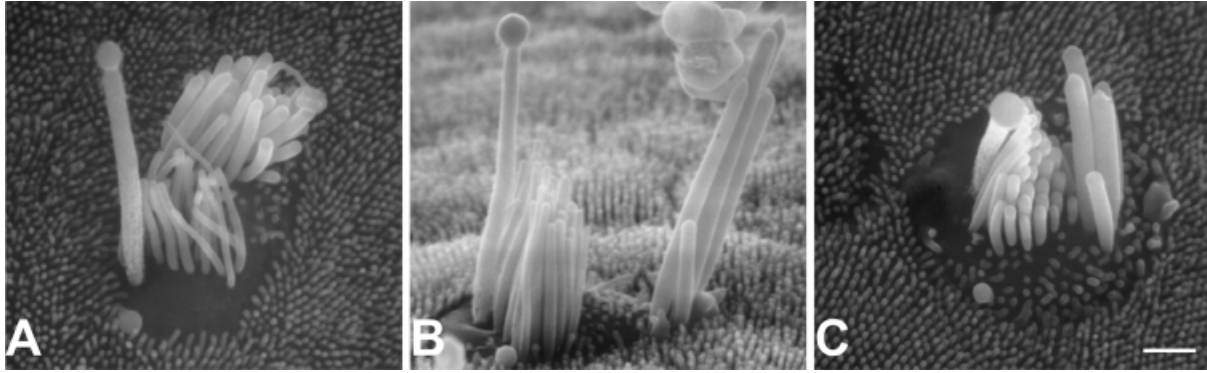


Figure 5 Scanning electron micrographs showing hair cells that have a complete, small, immature bundle alongside a remnant of a mature damaged hair bundle. Each micrograph shows the apical surface of one hair cell surrounded by microvilli on the surfaces of supporting cells. A fragment of a mature hair bundle comprised of tall, thick stereocilia that had formed and matured before the cell was damaged by the gentamicin treatment is present toward the top in (A) and to the right in (B) and (C). Note the close packing and the gradation in height of the stereocilia in the small bundles in (C). Scale bars: (A–C) 1 μm .

were found consistently only in the saccules that had recovered for 7 days. We noted that the surviving damaged bundles were usually associated with large apical surfaces [Fig. 4(B), thick arrow]. These cells correlate with images of bundleless hair cells with actin-rich cuticular plates that are seen in the FITC-phalloidin stained gentamicin-treated saccules. The declines in both the large bundles and the extruding bundles between 2 and 4 days led to a significant decrease in the total number of bundles between those time points. In contrast to the decline in numbers of large and extruding bundles, the number of small, immature bundles averaged only 1 per 10,000 μm^2 at 2 and 4 days, but increased to 15 per 10,000 μm^2 by 7 days [Fig. 4(C)]. The significant increase of small hair bundles between 4 and 7 days ($p < .001$; t test) is responsible for the increase in the total hair bundles observed at 7 days [Fig. 4(D)]. Because these cultures were maintained in 25 μM aphidicolin from the start of the gentamicin treatment this represents a significant level of recovery in the absence of cell proliferation.

Each of the small hair bundles observed contained a single kinocilium and many short, thin stereocilia [Fig. 4(C)]. The small bundles resembled bundles in embryonic ears and in guinea pig utricles recovering from gentamicin treatment (Forge et al., 1993). Some of the small bundles appeared to have arisen in pairs, where two bundles were close together and had small stereocilia of similar size [Fig. 4(B), double arrow]. The appearance of the pairs is particularly interesting because DNA replication was blocked from the end of the gentamicin treatment, which would prevent cells from progressing through S-phase after that point.

The occurrence of pairs suggests that some supporting cells might reside in G2 of the cell cycle and then, given the right stimulus, may re-enter the cycle and complete mitosis. Most small bundles, however, appeared to have arisen singly [Fig. 4(A)].

Unexpected evidence that mature pre-existing hair cells can regrow new bundles came from detailed SEM examinations of two saccules that were fixed 7 days after the gentamicin treatment. That ultrastructural analysis revealed hair cells that appeared to be regrowing a new bundle beside the damaged remnant of a mature bundle. A small, complete, but immature-appearing, hair bundle and a small group of taller, distinctly thicker stereocilia occurred at opposite poles of the same surface in 10 hair cells in one saccule and in 12 in the other [Fig. 5(A–C)]. The stereocilia in the small bundles on these cells averaged $0.2 \pm 0.01 \mu\text{m}$ in thickness and $2.2 \pm 0.2 \mu\text{m}$ in length (mean \pm S.E.M., $n = 38$). The larger stereocilia were significantly thicker, $0.36 \pm 0.04 \mu\text{m}$, and longer, $3.6 \pm 0.4 \mu\text{m}$ ($n = 18$, $p < .001$, two tailed t test). The number, the close packing, and the gradation in height of the stereocilia in the small bundles on the surfaces of these cells were consistent with those observed in the small bundles on neighboring cells [see Fig. 4(A–C)]. Such cells were observed only in saccules that had recovered for 7 days after the gentamicin treatment.

DISCUSSION

Moderate concentrations of aminoglycoside antibiotics are known to readily kill hair cells and when that

occurs in species that are capable of regeneration those treatments evoke massive proliferation of cells (Lippe et al., 1991). In our experiments, however, low concentrations of gentamicin for 16–18 h were found to have a range of effects on hair cells, from almost no change in morphology, to loss of the hair bundle and, in some cases, death of the cell. Time-lapse recordings and two-photon fluorescence time series showed the apical surfaces of some hair cells separating from the cell bodies at a point of constriction beneath the apical surface. Gentamicin damage may cause the cortical cytoskeletons of hair cells or the neighboring supporting cells to constrict at the site of the apical junctions between those cells in a manner akin to a purse-string mechanism. We observed cytoplasmic fingers of supporting cells protruding into the hair cells a short distance beneath the apical surface. In hair cell epithelia, myosins are located in the vicinity where the constriction occurs (Hasson et al., 1997) and might cause antiparallel filaments to slide together within the circumferential ring of actin near the adherens junctions, thereby driving bundle loss in some hair cells. Such a mechanism appears analogous to epithelial healing in the chick embryo where an actin cable forms at the edges of the wound followed by purse-string closure (Martin and Lewis, 1992). Structures similar to the cytoplasmic fingers described here have been observed in organ of Corti explants (Sobkowicz et al., 1997). The occurrence of bundleless hair cells that appeared to retain the cuticular plate (i.e., blackholes in SEM views and bundleless HCS-1 positive cells with cuticular plates) and the splitting of the cuticular plate and partial loss of the hair bundle that we observed in other cells, suggest that other mechanisms besides apical constriction can also contribute to antibiotic-induced loss of hair bundles. Progressive stages in the reorganization of actin bands and the formation of scars at and beneath the apical surface have been described previously in association with the loss of entire hair cells after aminoglycoside treatment of bullfrog sacculles (Baird et al., 1996) and guinea pig organs of Corti (Leonova and Raphael, 1997).

Time-lapse recordings revealed that subsequent to separation of the hair cell apices from the cell bodies many hair cells were phagocytosed by macrophages. However, other bundleless hair cells remained in the epithelium for the duration of the recordings. Two-photon microscopy confirmed that vitally labeled hair cells that had lost their apical poles survived for at least 6 days without visible contact with the epithelial surface. Immunocytochemical labeling of gentamicin-treated cultures fixed at different time points provided

further evidence that bundleless antibody-positive hair cells survived within the epithelium for 7 days.

SEM at 2 days showed stages in the initial loss of hair bundles from the surface of the epithelium. At 4 days the total number of hair bundles was reduced to less than one-third of those present at 2 days. By 7 days after the gentamicin treatment, a dramatic appearance of small bundles resulted in a two-fold increase from the total number of hair bundles that was present at 4 days. This occurred under conditions where DNA replication was blocked by aphidicolin. Together, the evidence from time-lapse recordings, two-photon microscopy, and immunocytochemistry indicated that hair cells could lose their hair bundles and survive as bundleless cells for 7 days. The evidence from SEM tracked the appearance of numerous small hair bundles and provided ultrastructural views of the preceding loss of mature bundles [Fig. 6(A)].

Perhaps most significantly, we observed a subset of the post-treatment hair cells that appeared to retain remnants of a mature, damaged bundle beside a complete, small, immature bundle on the same cell surface. It seems likely that such cell surfaces may have arisen after the apical bundle splitting that we observed in some time-lapse recordings [Fig. 2(F–H)]. The simplest explanation for such observations is that the cells were fixed while in the process of regrowing a new hair bundle adjacent to the remnant of a mature pre-existing bundle that had been damaged by the gentamicin treatment that ended a week prior to fixation [Fig. 6(B)].

Replacement of the hair bundle may be dependent upon loss of the cuticular plate, a rigid cytoskeletal specialization comprised of filamentous actin, spectrin, and tropomyosin that lies just beneath the plasma membrane under the hair bundle. The observation that new, small hair bundles can form adjacent to partial remnants of a mature bundle and underlying cuticular plate is consistent with the hypothesis that an *intact* cuticular plate inhibits replacement of lost hair bundles (Corwin and Warchol, 1991). The additional observation that a subset of surviving, bundleless hair cells that have large, flat apical surfaces does not show signs of new bundles even 7 days after treatment is also consistent with that hypothesis. Ultrastructural investigations have shown that the cuticular plate forms after the hair bundle has become fully organized during normal development (Tilney et al., 1992), although the molecular constituents of the plate appear in the vicinity of the future plate at an early stage (Yishida et al., 1998).

Observations from damaged hearing organs in birds initially led to the hypothesis that supporting cells can convert directly into hair cells without an

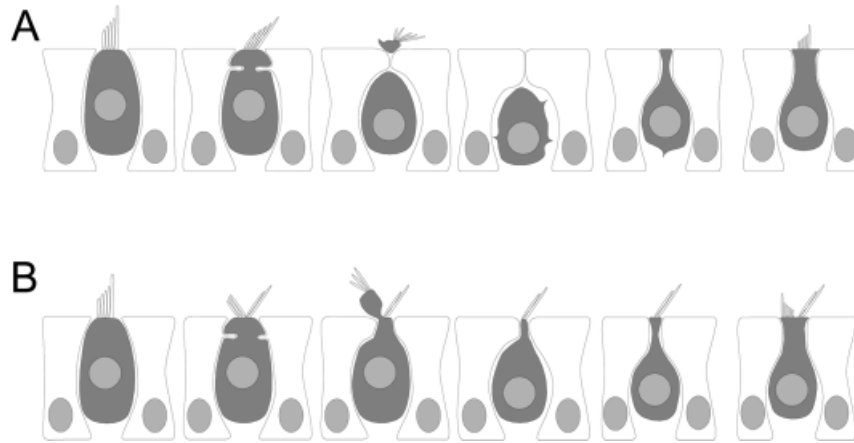


Figure 6 A model of hair bundle loss and replacement. (A) Repair process in hair cells (grey) that completely lose their bundles and survive as bundleless cells. After treatment with a low concentration of gentamicin, some hair bundles separate from the cell body. The apical parts of adjacent supporting cells (white) move into the region previously occupied by the apical part of the hair cell. Beneath the epithelial surface, bundleless hair cells descend towards the basal lamina. Bundleless hair cells are hypothesized to grow back to the apical surface of the epithelium. New hair bundles grow at the surface of the recovering hair cells. (B) Repair process in cells that lose only part of their apical surface and retain a damaged bundle. In some cases the hair bundles split in two and only part of the fractured bundle is extruded. New hair bundles grow at the surfaces of the cells with partially damaged bundles.

intervening cell division (Raphael and Miller, 1991; Adler and Raphael, 1996; Roberson et al., 1996). Similar hypotheses have been proposed to account for recovery in gentamicin-damaged vestibular organs of guinea pigs (Li and Forge, 1997) and in mitotically blocked bullfrog ears (Baird et al., 1993). Our observations cannot rule out the occurrence of such a conversion process, but the repair process we have described could account for nonproliferative recovery without the requirement for supporting cells to convert directly into sensory cells.

The intracellular repair and replacement of hair bundles we have described may also occur in the hearing and balance organs of mammals (Li and Forge, 1997; Sobkowicz et al., 1997; Zheng et al., 1999). Bundleless hair cells have been reported in a TEM study of embryonic organ of Corti explants after laser lesioning (Sobkowicz et al., 1997) and in neonatal rat utricles after gentamicin treatment *in vitro* (Zheng et al., 1999). In the latter there was a small, but significant, increase in bundle numbers over 11 days of recovery after gentamicin treatment (Zheng et al., 1999). Serial-section electron microscopy has shown that bundleless hair cells survive in the cochleas of humans with Menière's syndrome, a chronic condition characterized by episodes of extreme vertigo and progressive hearing loss (Nadol and Thornton, 1987; Nadol et al., 1995). Damaged, but surviv-

ing, hair cells may be found after systemic treatments where the levels of aminoglycosides are sufficiently weak as to not kill the animals from nephrotoxicity. Taken together, the observations suggest the possibility that loss and replacement of hair bundles may occur in humans and could potentially contribute to previously unexplained delayed recovery of auditory and vestibular sensitivity in mammals after treatments with ototoxic antibiotics (Black et al., 1987; Nicol et al., 1992; Meza et al., 1992). Such cellular repair might also explain delayed recovery of hearing thresholds after certain types of noise exposure, a phenomenon that is reported to continue for days (Mills et al., 1970). The replacement we describe provides a route for hair cell recovery that is independent of the production of new cells. A greater understanding of this repair mechanism might provide a pathway for therapeutic intervention in some cases of deafness and balance dysfunction.

We thank K. Karimi, D. Lenzi, P.R. Lambert, K. Lee, G.P. Richardson, A. Forge, R. Baird, P. Steyger, and I.J. Russell for helpful discussions. We are particularly grateful to B. Xia and J.E. Finley for technical assistance and characterization of the HCS-1 monoclonal antibody, and to B. Sheppard and J. Redick for superb assistance in electron microscopy. J.R.M. is a Howard Hughes Medi-

cal Institute Predoctoral Fellow. J.E.G is a Royal Society University Research Fellow.

REFERENCES

- Adler HJ, Raphael Y. 1996. New hair cells arise from supporting cell conversion in the acoustically damaged chick inner ear. *Neurosci Lett* 205:17–20.
- Ashmore J, Gale J. 2000. The cochlea. *Curr Biol* 10:R325–327.
- Baird RA, Steyger PS, Schuff NR. 1996. Mitotic and non-mitotic hair cell regeneration in the bullfrog vestibular otolith organs. *Ann NY Acad Sci* 781:59–70.
- Baird RA, Torres MA, Schuff NR. 1993. Hair cell regeneration in the bullfrog vestibular otolith following aminoglycoside toxicity. *Hear Res* 65:164–174.
- Black FO, Peterka RJ, Elardo SM. 1987. Vestibular reflex changes following aminoglycoside induced ototoxicity. *Laryngoscope* 97:582–586.
- Corwin JT. 1981. Postembryonic production and aging in inner ear hair cells in sharks. *J Comp Neurol* 201:541–553.
- Corwin JT. 1983. Postembryonic growth of the macula neglecta auditory detector in the ray, *Raja clavata*: continual increases in hair cell number, neural convergence, and physiological sensitivity. *J Comp Neurol* 217:345–356.
- Corwin JT. 1985. Perpetual production of hair cells and maturational changes in hair cell ultrastructure accompany postembryonic growth in an amphibian ear. *Proc Natl Acad Sci USA* 81:3911–3915.
- Corwin JT, Oberholtzer JC. 1997. Fish n'chicks: model recipes for hair cell regeneration? *Neuron* 19:951–954.
- Corwin JT, Warchol ME. 1991. Auditory hair cells: structure, function, development and regeneration. *Ann Rev Neurosci* 14:301–333.
- Corwin JT, Warchol ME, Saffer LD, Finley JE, Gu R, Lambert PR. 1996. Growth factors as potential drugs for the sensory epithelia of the ear. In: Bock GR, and Whelan J, editors. Growth factors as drugs for neurological and sensory disorders. Ciba Foundation Symposium 196. Chichester: Wiley, p 167–187.
- Diaz ME, Varela-Ramirez A, Serrano EE. 1995. Quality, bundle types, and distribution of hair cells in the sacculus of *Xenopus laevis* during development. *Hear Res* 91:33–42.
- Finley et al. 1997. *Abstr Assoc Res Otolaryngol* 20:134.
- Flock Å, Cheung HC, Flock B, Utter G. 1981. Three sets of actin filaments in sensory cells of the inner ear. Identification and functional orientation determined by gel electrophoresis, immunofluorescence and electron microscopy. *J Neurocytol* 10:133–147.
- Forge A, Li L, Corwin JT, Nevill G. 1993. Ultrastructural evidence for hair cell regeneration in the mammalian ear. *Science* 259:1616–1619.
- Gale JE, Meyers JR, Corwin JT. 2000. Solitary hair cells are distributed throughout the extramacular epithelium in the Bullfrog's sacculle. *JARO* 1:172–182.
- Harris WA, Hartenstein V. 1991. Neuronal determination without cell-division in *Xenopus* embryos. *Neuron* 6:499–515.
- Hasson T, Gillespie PG, Garcia JA, MacDonald RB, Zhao YD, Yee AG, Mooseker MS, Corey DP. 1997. Unconventional myosins in inner-ear sensory epithelia. *J Cell Biol* 137:1287–1307.
- Hudspeth AJ. 1989. How the ears works work. *Nature* 341:397–404.
- Lambert PR. 1994. Inner ear hair cell regeneration in a mammal: identification of a triggering factor. *Laryngoscope* 104:701–707.
- Leonova EV, Raphael Y. 1997. Organization of cell junctions and cytoskeleton in the reticular lamina in normal and ototoxically damaged organ of Corti. *Hear Res* 113:14–28.
- Li L, Forge A. 1997. Morphological evidence for supporting cell to hair conversion in the mammalian utricular macula. *Int J Dev Neurosci* 15:433–446.
- Li L, Nevill G, Forge A. 1995. Two modes of hair cell loss from the vestibular sensory epithelia of the guinea pig. *J Comp Neurol* 355:405–417.
- Liberman MC, Dodds LW. 1984. Single neuron labeling and chronic cochlear pathology. III. Stereocilia damage and alterations of threshold tuning curves. *Hear Res* 16:55–74.
- Lippe WR, Westbrook EW, Ryals BM. 1991. Hair cell regeneration in the chicken cochlea following aminoglycoside toxicity. *Hear Res* 56:133–142.
- Martin P, Lewis J. 1992. Actin cables and epidermal movement in embryonic wound-healing. *Nature* 360:179–183.
- Meza G, Solano-Flores LP, Poblano A. 1992. Recovery of vestibular function in young guinea-pigs streptomycin treatment - glutamate-decarboxylase activity and nystagmus response assessment. *Int J Dev Neurosci* 10:407–411.
- Mills JH, Gengel RW, Watson CS, Miller JD. 1970. Temporary changes of the auditory system due to exposure to noise for one or two days. *J Acoust Soc Am* 48:524–530.
- Nadol JB Jr. 1993. Hearing Loss. *N Engl J Med* 329:1092–1102.
- Nadol JB Jr, Adams JC, Kim JR. 1995. Degenerative changes in the organ of corti and lateral cochlear wall in experimental endolymphatic hydrops and human Menières-disease. *Acta Otolaryngol (Stockh) Suppl* 519:47–59.
- Nadol JB Jr, Thornton AR. 1987. Ultrastructural findings in a case of Menières-disease. *Ann Otol Rhinol Laryngol* 96:449–454.
- Nicol KM, Hackney CM, Evans EF, Pratt SR. 1992. Behavioural evidence for recovery of auditory function in guinea pigs following kanamycin administration. *Hear Res* 61:117–131.

- Periasamy A, Skoglund P, Noakes C, Keller R. 1999. An evaluation of two-photon excitation versus confocal and digital deconvolution fluorescence microscopy imaging in *Xenopus* morphogenesis. *Microsc Res Tech* 47:172–181.
- Popper AN, Hoxter B. 1984. Growth of the fish ear. 1. Quantitative analysis of hair cell and ganglion cell proliferation. *Hear Res* 15:133–142.
- Raphael Y, Miller J. 1991. *Soc Neurosci Abstr* 17:1214.
- Roberson DW, Kreig CS, Rubel EW. 1996. Light microscopic evidence that direct transdifferentiation gives rise to new hair cells in regenerating avian auditory epithelium. *Aud Neurosci* 2:195–205.
- Ruben RJ. 1967. Development of the inner ear of the mouse: A radioautographic study of terminal mitosis. *Acta Otolaryngol (Stockh) Suppl* 220:1–44.
- Sobkowicz HM, August BK, Slapnick SM. 1997. Cellular interactions as a response to injury in the organ of Corti in culture. *Int J Devl Neurosci* 15:463–485.
- Tilney LG, Tilney MS, DeRosier DJ. 1992. Actin-filaments, stereocilia, and hair-cells—how cells count and measure. *Ann Rev Cell Biol* 8:257–274.
- Warchol ME, Lambert PR, Goldstein BJ, Forge A, Corwin JT. 1993. Regenerative proliferation in inner ear sensory epithelia from adult guinea pigs and humans. *Science* 259:1619–1622.
- Yishida N, Rivolta M, Holley MC. 1998. Timed markers for the differentiation of the cuticular plate and stereocilia in hair cells from the mouse inner ear. *J Comp Neurol* 395:18–28.
- Zheng JL, Keller G, Gao WQ. 1999. Immunocytochemical and morphological evidence for intracellular self-repair as an important contributor to mammalian hair cell recovery. *J Neurosci* 19:2161–2170.